Steel and Composite Structures, *Vol. 29, No. 1 (2018) 39-51*
DOI: https://doi.org/10.12989/scs.2018.29.1.039

Position optimization of circular/elliptical cutout within an orthotropic rectangular plate for maximum buckling load

Prashant K. Choudhary [a] and Prasun Jana [*]

Department of Mechanical Engineering, Indian Institute of Technology (Indian School of Mines), Dhanbad-826004, India

(*Received February 9, 2018, Revised July 26, 2018, Accepted August 3, 2018*)

Abstract. Position of a circular or elliptical cutout within an orthotropic plate has great influence on its buckling behavior. This paper aims at finding the optimal position (both location and orientation) of a single circular/elliptical cutout, within an orthotropic rectangular plate, that maximizes the critical buckling load. We consider linear buckling of simply supported orthotropic plates under uniaxial edge loads. To obtain the optimal positions of the cutouts, we have employed a MATLAB optimization routine coupled with buckling computation in ANSYS. Our results show that the position of the cutout that maximizes the buckling load has great dependence on the material properties, laminate configurations, and the geometrical parameters of the plate. These optimal results, for a number of plate geometries and cutout sizes, are reported in this paper. These results will be useful in the design of perforated orthotropic plates against buckling failure.

Keywords: rectangular plate; orthotropic material; cutout; buckling analysis; optimization

1. Introduction

Thin-walled plate type structures made of orthotropic materials constitute very important structural components in many engineering applications, especially in aerospace, mechanical and civil industries. For efficient design purposes there is a need to introduce holes or cutouts into these structures. The presence of these cutout openings changes the stress distribution within these perforated structures and thereby results in variations in the internal stress distributions. Under excessive compressive loading these plate structures will undergo buckling instability which results in loss of structural stiffness and thereby reduction in the load bearing capacity of the structure (Leissa 1987, Zhang and Yang 2009, Larsson 1987), Nemeth 1988).

In this paper, we study linear buckling of a thin orthotropic rectangular plate that contains a single circular/elliptical cutout. The plate is simply supported at all four edges and subjected to uniform uniaxial in-plane compressive edge loads. Our aim is to employ a formal optimization algorithm to obtain the true optimal design parameters (e.g., location and orientation) of the cutout and maximize the critical buckling load.

We note that the existing literature (see below for a brief literature review) does talk about the influence of cutout position on the critical buckling load of orthotropic plates. However, to the best of our knowledge, no work seems to adopt a formal optimization scheme for determining the optimal location parameters in orthotropic plates that maximize the critical buckling load.

A common observation in the studies reported in the literature is that the location and orientation of cutout within the structure have been chosen first and then the buckling load has been obtained (Qablan *et al*. 2009, Narayana *et al*. 2013). In contrast to that, in this work, we have developed an optimization scheme for obtaining the optimal location and orientation of the cutout within a perforated orthotropic plate for maximum critical buckling load. The perforated plate is first modeled parametrically in finite element analysis software ANSYS for buckling load calculation and then these buckling results were coupled with a MATLAB optimization routine to find the true optimal cutout parameters. We note that for the computation of critical buckling load of the plate, with cutout at some arbitrary position, a finite element solution is only viable as the analytical solution in this case is either unavailable or intractable. Therefore, the novelty of the present work lies in the development of the MATLAB optimization scheme that interacts with the ANSYS buckling computation for orthotropic plate in each iteration and produces the optimal cutout position as final outcome of this optimization run.

Optimization study for the buckling of an isotropic plate having a single circular cutout has been published recently by one of the authors of this article (Jana 2016). In this paper, the study has been extended to the optimal design of both circular and elliptical cutouts within the orthotropic plates. We have considered both symmetric cross-ply $(0^{\circ}/90^{\circ})_{2s}$ and angle-ply $(30^{\circ}/-60^{\circ})_{2s}$ laminated plates. The study shows that the optimal position of cutout for the maximum buckling load has great dependence on the material properties, laminate sequence, geometrical parameters of the plate, and on the size of the cutouts. These optimal results are reported in this paper, using tables and graphs, for a number of plate geometries and cutout

*Corresponding author, Ph.D., Assistant Professor,
E-mail: prasunjana@gmail.com; prasun@aero.iitkgp.ac.in
[a] Ph.D. Student,
E-mail: prashantkumarchoudhary01@gmail.com

ISSN: 1229-9367 (Print), 1598-6233 (Online)

sizes. The results reported here are important from a design point of view and will be useful in the design of orthotropic plate against buckling failure.

2. Related prior work

The literature on buckling of rectangular plates is rich. Many studied are exclusively confined to isotropic plates (Komur and Sonmez 2008, Komur 2011, Seifi *et al*. 2017, Jana 2016). And several others discuss buckling behavior of orthotropic rectangular plates but without any cutout (Darvizeh *et al*. 2002, Aktas and Balcioglu 2014, Altunsaray and Bayer 2014, Lopatin and Morozov 2014, Baseri *et al*. 2016). However, we consider optimal design of cutouts within orthotropic plates and briefly review the relevant literature pertaining to the work presented in this article. Larsson (1987) used finite element method (FEM) to investigate the influence of a central circular hole on the buckling and post-buckling behaviour of square orthotropic plates subjected to uniaxial and biaxial compression. Nemeth (1988) studied experimentally the buckling behaviour of orthotropic rectangular symmetric angle-ply laminates with a circular cutout. Qablan *et al*. (2009) and Narayana *et al*. (2013) considered square/rectangular cutouts and performed multiple FEM analyses in ANSYS by positioning the cutout in some selected locations in order to find the location effect of the cutout on the buckling behavior of the orthotropic plates. Lin and Kuo (1989) studied the effects of circular cutouts on the critical buckling of symmetrically or anti-symmetrically laminated composite plates subjected to in-plane static loadings. They have used nine-node Lagrangian finite element technique for computing the critical loads. Lee *et al*. (1989) studied the buckling behaviour of an orthotropic plate, either with or without a central circular cutout. They investigated the influence of material orthotropy of the laminated plate on the buckling load by using finite element method. Srivatsa and Murty (1992) used classical lamination theory and FEM to obtain critical buckling load of laminated fibre reinforced plastic (FRP) square panel. They studied the effect of various design parameters including lay-up sequence, fibre orientation, cut out size, and different boundary conditions. Jain and Kumar (2004) used FEM to study the post-buckling response of symmetric square plate having a central cutout subjected to uniaxial compression. Ghannadpour *et al*. (2006) studied the buckling behaviour of rectangular symmetric cross ply laminates by using finite element analysis. They focused on the effect of a central cutout on the buckling performance of a rectangular plate. Mohammadi *et al*. (2006) investigated the effect of eccentric circular cutout on the pre-buckling and post-buckling stiffness of laminated composite plates. They also computed the effective width of compression loaded laminated composite plates based on non-linear finite element analysis. Baltaci *et al*. (2006) studied using FEM the buckling behaviour of laminated composite circular plates with circular hole and subjected to uniform radial load. Baba (2007) investigated numerically and experimentally the effect of various influencing parameters such as boundary condition, cutout shape, length-to-thickness ratio and ply orientation on the buckling behaviour of composite plates under in-plane edge compression. Baba and Baltaci (2007) used ANSYS to study the buckling behavior of symmetrically and anti-symmetrically laminated orthotropic plates with a central cutout. They also validated their results using experiments. Onkar *et al*. (2007) presented a stochastic finite element formulation which is based on the mean centered first order perturbation technique for analyzing the buckling behavior of laminated composite plate with circular cutout and having uncertain material properties. Zhong and Gu (2007) developed an exact buckling solution of simply supported symmetric cross-ply laminated orthotropic rectangular plates under linearly varying in-plane load. They used finite element analysis in ABAQUS to verify their result. Anil *et al*. (2007) used a 'simple higher order shear deformation theory' to incorporate the effect of pre-buckled stress on the stability analysis of composite laminated plates with and without rectangular cutouts under in-plane compressive loading. Komur *et al*. (2010) used finite element analysis in ANSYS to study the buckling characteristics of laminated composite plate with a centrally located elliptical/ circular cutout. They calculated the buckling load for different cutout sizes and their orientations. Kumar and Singh (2010) studied, using FEM, the effect of flexural boundary condition on buckling and post-buckling characteristics of laminated composites with cutout under uniform edge loads. The FEM formulation they used is based on the first order shear deformation theory along with the incorporation of geometric non-linearity. Rajanna *et al*. (2016) used finite element analysis to study the buckling behavior of perforated laminated panel subjected to uniform and nonuniform in-plane edge loads.

We now review some literatures that discuss optimization in composite plates. Walker (1999) studied the optimal design of symmetrically laminated rectangular plate with central circular cutouts for maximum buckling load. The author determined the fibre orientations optimally with the effect of bending-twisting coupling included. Spallino and Rizzo (2002) presented a multi-objective optimization based on Evolution Strategies to optimize the laminate sequence in the laminated composite structures. Adali *et al*. (2003) investigated the optimal design of symmetrical laminated composite plates subjected to biaxial compressive load. The author used anti-optimization approach to optimize ply angle for maximum buckling load. Sivakumar *et al*. (1998) used genetic algorithm (GA) to design an orthotropic plate in the presence of elliptical cutouts for optimum free vibration response. Zehnder and Ermanni (2006) introduced a methodology for the global optimization of real-world laminated composite structures using evolutionary algorithms. The authors validated their methodology by optimizing the stiffness of a sailing boat for a given weight and cost limits. Paluch *et al*. (2008) developed a procedure to combine finite element analysis and genetic algorithm to optimize composite structures with variable thickness. Topal and Uzman (2007) used modified feasible direction (MFD) method for optimum design of laminated composite plates with central circular hole to

maximize buckling load. They considered fibre orientations as design variables. Sharma *et al*. (2014) used Muskhelishvili's complex variable approach to optimize the laminate stacking sequence of perforated orthotropic plate subjected to in-plane edge loading.

From the above literature survey, we conclude that study towards finding the true optimal position of circular/ elliptical cutout within an orthotropic plate has not been reported yet. In the literature, it has been observed that the position of the cutout has not been considered as the design variable for the optimization studies. In most of these studies, the position of the cutout is chosen first and then the effects of the cutout on the buckling behaviour of the orthotropic plate have been studied. Therefore, in this paper, our objective is to develop a novel optimization technique that employs an iterative procedure for selection of the position of the cutout by using a widely accepted optimization algorithm such that the true optimal position of the cutout is obtained. The optimization routine is developed within MATLAB and is coupled with the finite element buckling computation in ANSYS. Details of the methodology and some interesting results are discussed below.

3. Scope of the study

In this study, the critical buckling load of the orthotropic plate is computed using the general purpose commercial finite element software ANSYS. The rectangular plate with length a, width b, thickness h, are considered to be simply supported at all four edges and subjected to uniform uniaxial compressive edge loads (N_0) along the x-direction. See Fig. 1 for the schematic of the plate. An elliptical cutout of major axis 2c and minor axis 2e is located at an arbitrary position (x_c, y_c) within the plate and is inclined by an angle (θ) with the x-axis. Note that the cutout will become circular when the ratio c/e is set to 1.

3.1 Material properties

In this work, both cross-ply $(0^\circ/90^\circ)_{2s}$ and angle-ply $(30^\circ/-60^\circ)_{2s}$ laminates are considered. The thickness of each layer in this eight-layer laminate is taken as 0.15 mm. The orthotropic material properties of the lamina used for the buckling analysis in this paper are shown in Table 1 (adopted from reference Jain and Kumar (2004), Ghannadpour *et al*. (2006)). In this table, E, G, and ν correspond to the Young's moduli, shear moduli, and Poisson's ratios respectively.

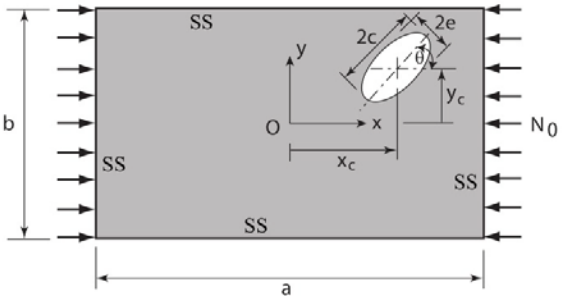

Fig. 1 Schematic of the uniaxially compressed orthotropic rectangular plate (length a, width b, and thickness h) containing an elliptical hole and having all edge simply supported (SS)

3.2 Buckling analysis

For the buckling analysis in ANSYS, four node SHELL181 elements have been used for the discretization of the plate. This element has six nodal degrees of freedom (translations in x, y, z-axes and rotations about the x, y, and z-axes). This element is used for the analysis of thin to moderately thick plates and shells as it considers transverse shear deformations (ANSYS Inc. 2015). See Section 3.3 for a validation study with already published results.

In ANSYS, a geometric model of the perforated plate is first generated and then the structure is meshed using SHELL181 elements. In order to get accurate buckling results, mesh convergence study has been carried out (details not reported here). A relatively finer mesh near the cutout geometry is used for better accuracy. See Fig. 2 for a typical finite element mesh used for the plate having an elliptical cutout at some arbitrary location. The boundary condition used in the analysis is simply supported at all four edges. For simulating simply supported boundary condition, displacements in the z direction along all the four edges are restrained. Additionally, x and y displacements for one node on the $x = -a/2$ edge and y displacement of a node on the $x = a/2$ edge are restrained in order to prevent only the rigid body motion of the plate.

Note that the numerical results computed from the linear (eigenvalue) buckling analysis in ANSYS are some scaling factors (say SF) that has to be multiplied to the loads

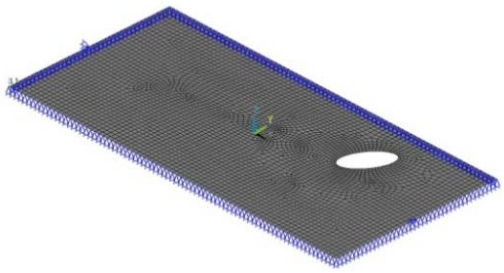

Fig. 2 A typical finite element meshes of the laminated orthotropic plate with an elliptical cutout at some arbitrary location

Table 1 Mechanical properties (adopted from Jain and Kumar 2004, Ghannadpour *et al*. 2006) of the lamina used for the results reported in this paper

Mechanical properties	Values
E_1	130.0 GPa
$E_2 = E_3$	10.0 GPa
$G_{12} = G_{13}$	5.0 GPa
$\nu_{12} = \nu_{13}$	0.35
ν_{23}	0.49

applied in the FE model in order to get the buckling instability of the structure. Therefore, the total critical buckling load of the plate will be calculated as N_{xcr} = SF × N_0. In this paper, we focus on the first instability of the orthotropic plate and compute the first critical buckling load.

3.3 Validation of buckling load computation

To validate our buckling load computation, we compare our results with some already published literature (Jain and Kumar 2004, Ghannadpour *et al*. 2006). For this comparison study, we have considered the same plate dimensions, material properties, boundary conditions and laminate sequences as taken in these references. Table 2 shows the comparison of the first nondimensional critical buckling loads $\bar{N}_{xcr} = N_{xcr}\, b^2/(E_2 h^3)$. From the table it can be seen that our results are in good agreement with the published results. Slight mismatch seen in case of Jain and Kumar (2004) may be because of their less converged results with coarse mesh size whereas our reported numbers are due to finer mesh size thereby resulting more accurate values.

3.4 Determination of optimal cutout position

Linear elastic buckling analyses of the perforated orthotropic plate have been carried out for a number of cases after varying few design parameters such as size and shape of the cutout, location and orientation of the cutout, and the aspect ratio of the plate. In our analysis, the width b of the plate is taken as 1 m whereas the the length is varied as the aspect ratio (AR = a/b) of the plate changes. As an example, the length a becomes 1.5 m when AR is set to 1.5. For the circular cutout, three cutout sizes of radius 0.1 m, 0.15 m and 0.2 m are considered. For the elliptical cutout, the ratio c/e is set to 2. We have considered three elliptical cutouts having the same area of the previously mentioned circular cutouts. Additionally, as a design limitation, a minimum margin of 0.05 m between the edges of the cutout and the plate is assumed. This will add a constraint to our optimization problem. For all of these cases the finite element buckling computations in ANSYS are coupled with a MATLAB optimization routine and the optimal positions of the circular/elliptical cutout are obtained. Details of the optimization routine and the optimal results are discussed below.

Table 2 Comparison of nondimensional buckling load $\bar{N}_{xcr} = N_{xcr}\, b^2/(E_2 h^3)$ with existing literature results (Jain and kumar 2004, Ghannadpour *et al*. 2006)

Cutout shape and size	Laminate sequence	Non-dimensional buckling load	
		Present study	Literature values
Circular cutout $c = e = 0.25b$	$[(\pm 45^\circ/0^\circ/90^\circ)_5]_S$	13.59	13.84 (Jain and Kumar 2004)
	$[(0^\circ/90^\circ)_2]_S$	6.40	6.39 (Ghannadpour *et al*. 2006)
Elliptical cutout $c = 0.25b$; $e = 0.5c$	$[(\pm 45^\circ/0^\circ/90^\circ)_5]_S$	12.74	13.05 (Jain and Kumar 2004)
	$[(0^\circ/90^\circ)_2]_S$	7.64	7.63 (Jain and Kumar 2004)

4. Optimization routine

For the optimization, the objective function that is the first critical buckling load of the orthotropic plate is considered as a function of the position (x_c, y_c) and orientation (θ) of the cutout. Therefore, x_c, y_c, and θ are the three input parameters (p) in this optimization process. For obtaining the optimal position of the cutout systematically and accurately, we develop an optimization routine in MATLAB that uses the ANSYS buckling computation iteratively and provide the optimal results as final output. The execution of the entire optimization process is done in three modules as described below. See Fig. 3 for the flow diagram of these modules.

4.1 Module 1: FE computing of buckling load

ANSYS Parametric Design Language (APDLs) along with the automatic mesh generation techniques available in ANSYS has been used for generating the parametric finite element model for the buckling analysis. ANSYS APDLs that has been used for a typical case is shown in Appendix A. For a given plate dimension and cutout size and shape, this APDLs accept an input parameter, i.e., $p = \{x_c, y_c, \theta\}$ and returns N_{xcr} that has to be used in the evaluation of the objective function in Module 2.

4.2 Module 2: Input parameter and definition of objective function

Module 2 consists of two things: The input design

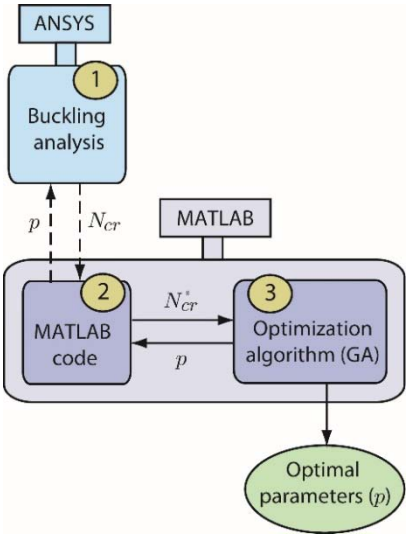

Fig. 3 Schematic of the flow diagram used in the optimization routine for computing the optimal position of the cutout for the maximum buckling load

parameters (p) and the objective function (N^*_{xcr}). These are defined using a MATLAB code. For a given structural configurations, this module accept the input parameters $p = \{x_c, y_c, \theta\}$ and feed it to the module 1 to obtain the scalar N_{xcr} that has to be used in the objective function (N^*_{xcr}) evaluation. Note that the output N_{xcr} from ANSYS is a positive scalar number that represents the first critical buckling load and we would like to maximize it. Therefore, to use some in-built optimization algorithm already available within MATLAB, we convert this maximization problem to a regular minimization problem. We do that by making $N^*_{xcr} = -N_{xcr}$. We also emphasize here that this evaluation of N^*_{xcr} are carried out for every iteration of the optimization run used in module 3.

4.3 Module 2: Input parameter and definition of objective function

Module 3 is for the optimization process for finding the optimal parameters. In this module, a suitable optimization algorithm (here, genetic algorithm (GA)) available within MATLAB is selected. GA has become a popular and robust tool for function optimization with multiple parameters. One advantage of this algorithm is that it does not require differentiability of the objective function. It works with function evaluations at discrete points. The algorithm is based on the concepts of natural selection and genetics (Goldberg 2005).

In MATLAB, following syntax is used for the optimization.

[Xopt, f (Xopt)] = ga (@objectivefun, nvars, options)

Here, @objectivefun is the objective function which has to be minimized. In our case it is N^*_{xcr}. nvars is the number of variables (i.e., x_c, y_c, *and* θ) for the optimization. Options are to handle the design constraints. The final outputs from this optimization run are given by Xopt as the optimal point and f (Xopt) as the corresponding value of the objective function at that optimal point.

There are various GA parameters that play important roles in finding the optimal value of the objective function. Thus, accuracy of the optimization result can be improved by adjusting these parameters. We finalize these parameters based on convergence study via multiple GA runs with different values of GA parameters such as population size, crossover probabilities etc. See Table 3 for some of these selected GA parameters for this study.

Table 3 Parameter used in genetic algorithm (GA) optimization runs

Population size	50
No. of variable	3(x_c, y_c and θ)
Population type	Double vector
Selection Method	Stochastic uniform
Elite count	2.5
Mutation function	Constraint dependent
Crossover function	Constraint dependent
Probability of crossover	0.8
No. of generation	100
Stall generation	60

5. Results and discussions

In this section, the optimal results obtained from above optimization routine are discussed. For better understanding of the results, the buckling loads of the perforated plates are normalized with respect to the corresponding buckling load of the unperforated plate. Thus, the normalized buckling factor (NBF) is defined as

$$\text{NBF} = \frac{\bar{N}_{xcr}}{N^0{}_{xcr}}, \tag{1}$$

Where $\bar{N}_{xcr}$ and $N^0{}_{xcr}$ are the critical buckling load of orthotropic plate with and without the cutout, respectively. The analytical formula for computing $N^0{}_{xcr}$ for a symmetric cross-ply laminated plate is given by

$$N^0{}_{xcr} = \pi^2 \left(D_{11} \left(\frac{m}{\pi}\right)^2 + 2(D_{12} + 2D_{66}) \left(\frac{1}{b}\right)^2 + D_{22} \left(\frac{a}{m}\right)^2 \left(\frac{1}{b}\right)^4 \right) \tag{2}$$

where m is the number of half waves along x-direction and D_{ij} are the flexural stiffness coefficients of the orthotropic plate. For a symmetric angle-ply laminated plate, the presence non-zero bending-twisting coupling coefficients D_{16} and D_{26} makes it practically impossible to get a closed form expression for $N^0{}_{xcr}$ (Reddy 2003). Therefore, for the angle-ply laminated plates, we use ANSYS computed buckling results of the unperforated plate in order to compute the normalized buckling factor (NBF).

In the following subsections, we first consider circular cutout and discuss results for both cross-ply $(0^\circ/90^\circ)_{2s}$ and angle-ply $(30^\circ/-60^\circ)_{2s}$ laminates. Afterwords, results for an elliptical cutout are reported. Subsequently, influences of cutout size on the optimal results are highlighted. We finally end this section with the discussion on the effect of material orthotropy on these optimal results.

5.1 Circular cutout

5.1.1 Cross-ply laminate

We first consider cross-ply $(0^\circ/90^\circ)_{2s}$ laminated plate having a circular cutout of radius $c = e = 0.1$ m. The plate width is set to 1 m and the aspect ratio (AR = a/b) is varied from 1 to 4.5. Additionally, a minimum margin of 0.05 m between the edge of the cutout and the plate is considered as a design constraint. For all these cases, the optimal center locations (x_c , y_c) of the circular cutout are obtained using above optimization routine. Note that the orientation (θ) will become a design variable for an elliptical cutout but not for the circular cutout which is considered here.

Considering the fact that the plate is symmetric about both the x and y-axes, we only report the optimal (x_c , y_c)

values in the first quadrant of the plate that correspond to the maximum critical buckling load. However, one should note that from these optimal (x_c , y_c) values three different set of values for the three other quadrants can also be obtained which will produce the same optimal results.

Fig. 4(a) shows the optimal locations of the cutout for various values of the plate aspect ratios. The optimal results are also presented in a tabular form in Table 4 in Appendix B.

Table 4 actually presents four sets of optimal results; the first data set corresponds to this present case and the other three data sets are relevant to the cases discussed afterwords. From Fig. 4(a) it is seen that for AR = 1 to 1.7 the optimal x_c is near the $x = a/2$ edge (leaving the minimum margin) of the plate and the optimal y_c values are somewhere between the x-axis and the $y = b/2$ edge. As the aspect ratio increases from AR = 1.8 to 2.8, optimal center locations of the cutout move from 'near the edge' to the

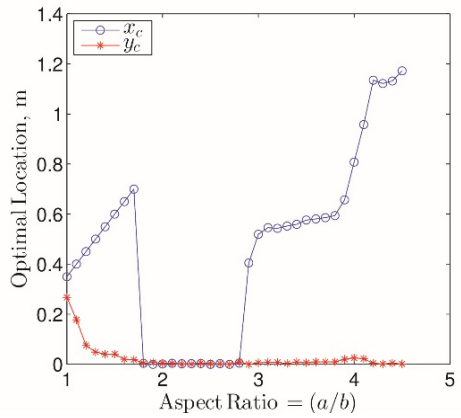

(a) Optimal locations (x_c, y_c) of circular cutout

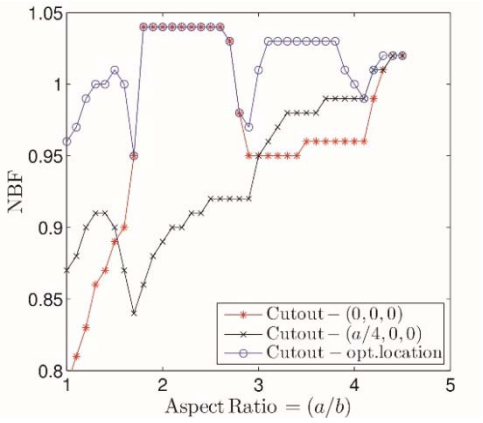

(b) Normalized buckling factor (NBF) for three different positions of the circular cutout

Fig. 4 Optimization results of cross-ply $(0°/90°)_{2s}$ laminated plate

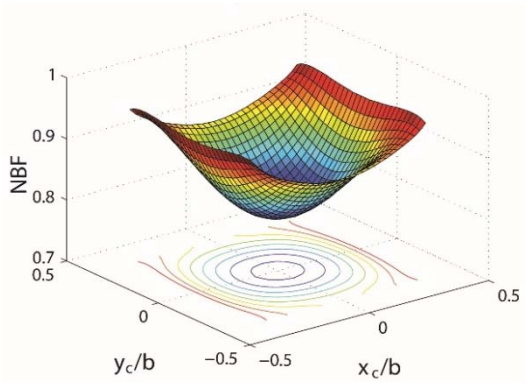

(a) Aspect ratio = 1.0

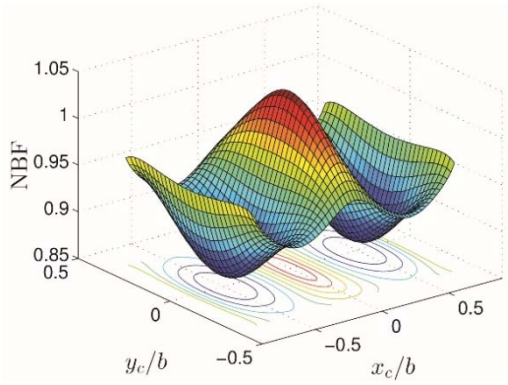

(b) Aspect ratio = 1.8

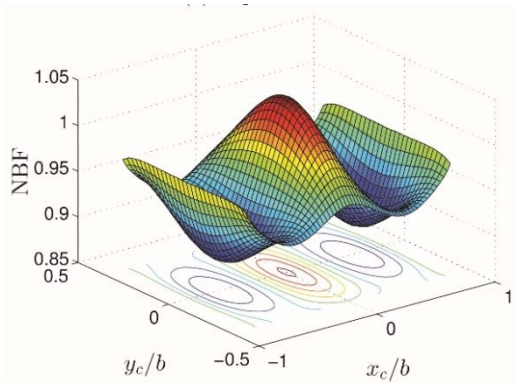

(c) Aspect ratio = 2.0

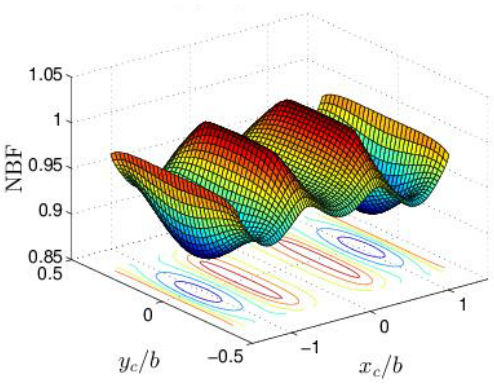

(d) Aspect ratio = 3.0

Fig. 5 Surface plot of the normalized buckling factor (NBF) against several positions (x_c, y_c) of the circular cutout for a number of aspect ratios of the plate

'center' of the plate. Interestingly, for AR = 2.9 to 4.5 the optimal y_c locations remain mostly on the longitudinal center line (x-axis) but the optimal x_c locations remain between the center and the $x = a/2$ edge of the plate as shown by the curve in Fig. 4(a).

Fig. 4(b) shows the normalized buckling factor (NBF) for three different cases. In the first case, the cutout is placed at the center of the plate. The second case is for the cutout kept at (a/4, 0) position. And, in the third cases, the cutout is placed at the optimal locations as obtained in Fig. 4(a). Firstly, these plots show that the cutout position has profound effect on the critical buckling load of the orthotropic plate. Secondly, the figure confirms (at least partially) that the buckling load at the optimal location always maintains a higher value. To get a more clear understanding of the above optimal results, we show four surface plots in Fig. 5. These surface plots, for a given plate aspect ratio, are generated after carrying out number of buckling simulations by varying the cutout location all along the plate. Fig. 5 shows that for each plate aspect ratio the first critical buckling load is a well-defined function of the position of the cutout and an optimal location can be found for which the critical buckling load will be maximum. Four surface plots in Fig. 5 for different aspect ratios also indicate that the optimal location changes as the aspect ratio of the plate changes. And these optimal results for a number of aspect ratios were shown in Fig. 4(a).

In Fig. 6, we show the first buckling mode shapes of four different plate aspect ratios having the circular cutout located at its optimal position. These plots show that the optimal position of the cutout for AR = 2.0 remains on the nodal lines whereas for other three cases it remains far from the nodal lines. Therefore, the optimal positions of the cutouts may not be intuitively guessed by some judgments rather it should be obtained systematically by using some optimization method as illustrated in this article.

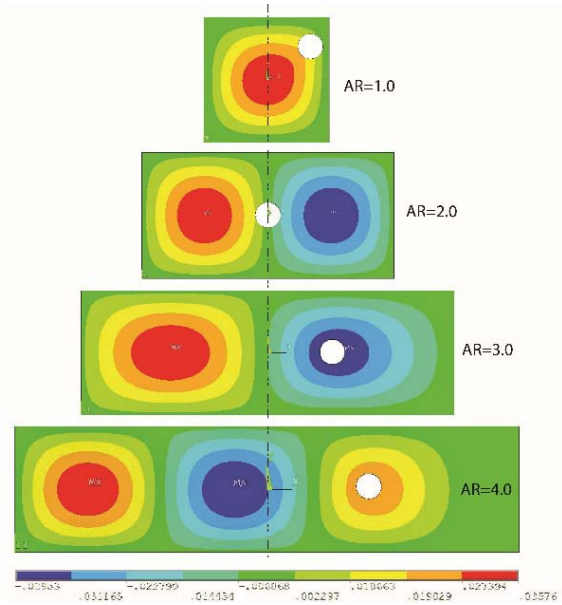

Fig. 6 First buckling modes of four different plate aspect ratios at their optimal configurations. The color bar represents the out-of-plane displacements

5.1.2 Angle-ply laminates

We now consider angle-ply $(30^\circ/-60^\circ)_{2s}$ laminated plate and perform similar optimization studies. The dimensions of the circular cutout and the plate are taken exactly same as described above for cross-ply $(0^\circ/90^\circ)_{2s}$ laminated plate.

The optimal locations (x_c, y_c) of the circular cutout within this angle-ply $(30^\circ/-60^\circ)_{2s}$ laminated plate for various values of the plate aspect ratios are shown in Fig. 7(a). See also Table 4 in Appendix B for the tabulated results. Fig. 7(a) shows that for AR = 1.2 to 4.5 the optimal y_c locations are very close to zero. This means that the optimal cutout center remains mostly on the x-axis. However, the optimal x_c locations vary significantly along this x-axis as the aspect ratio of the plate changes. For AR = 1 to 1.5, the optimal x_c is near the $x = a/2$ edge of the plate. The optimal x_c locations shift from the edge to the center of the plate for AR = 1.6 to 2.6. As AR increases from 2.7 to 4.5, the optimal x_c values turn out to be between the center and the $x = a/2$ edge of the plate as depicted by the curve in Fig. 7(a).

To show that the optimal results shown in Fig. 7(a) correspond to the maximum critical buckling loads normalized buckling factor (NBF) for three different cutout locations are shown in Fig. 7(b). This figure indicates that buckling loads at the optimal locations always maintain higher values.

5.2 Elliptical cutout

This section discusses the optimal results for an elliptical cutout. In this case, the orientation (θ) of the cutout along with the center position (x_c, y_c) plays a significant role in determining the maximum buckling load. We consider both cross-ply $(0^\circ/90^\circ)_{2s}$ and angle-ply $(30^\circ/-60^\circ)_{2s}$ laminated plates. The dimension of the elliptical cutout is taken as c = 0.141 m with $e = 0.5c$, which makes the cutout area same of a circular cutout of radius 0.1 m. The width of the plate is set to 1 m and the plate aspect ratio (AR = a/b) is varied from 1 to 4.5. A minimum margin of 0.05 m between the edge of the cutout and the plate is also taken as design constraint. For these cases, the optimal positions (x_c, y_c, *and* θ) of the elliptical cutout are obtained using the optimization routine as depicted in Section 4.

5.2.1 Cross-ply laminate

Fig. 8(a) shows the optimal locations (x_c, y_c) of the elliptical cutout within the cross-ply $(0^\circ/90^\circ)_{2s}$ laminated plate for various values of the plate aspect ratios whereas Fig. 8(b) represents the corresponding optimal values. The optimal results are also shown in Table 4 in Appendix B.

From Fig. 8, it is seen that for AR = 1 to 1.6, the optimal x_c is near the $x = a/2$ edge, the optimal y_c values are between the x-axis and the $y = b/2$ edge, and the corresponding values are somewhere between 125° to 140°. However, for AR = 1.7 to 4.5, the optimal becomes more or less 90° and the corresponding optimal center locations are as shown in Fig. 8(a). In this case, we see that the optimal x_c values shift twice to the center of the plate: for AR = 1.7 to 2.7 and again for AR = 4.3 to 4.5. One more interesting point to observe from these results is that for long cross-ply

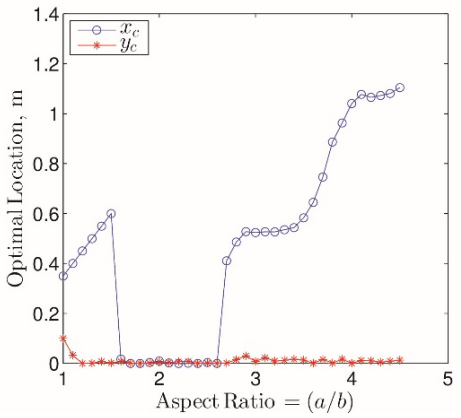

(a) Optimal locations (x_c, y_c) of circular cutout

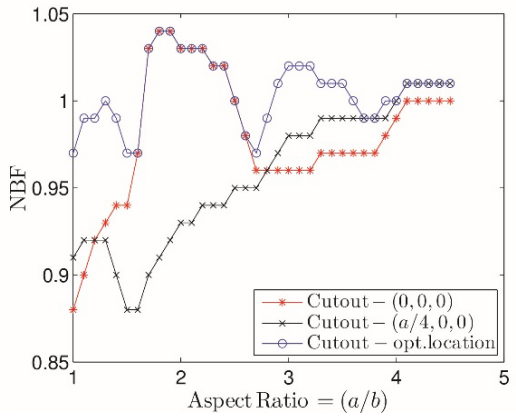

(b) Normalized buckling factor (NBF) for three different positions of the circular cutout

Fig. 7 Results for angle-ply (30°/-60°)$_{2s}$ laminated plate

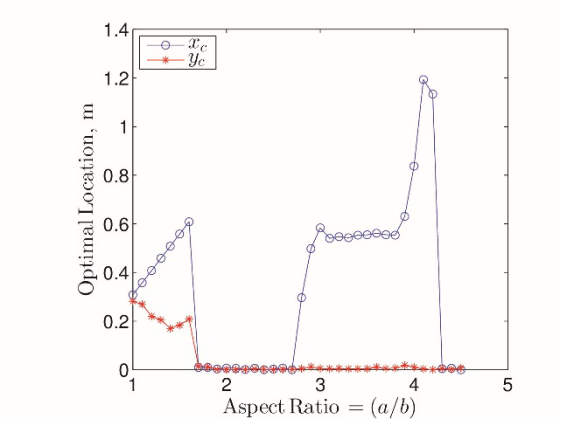

(a) Optimal center locations (x_c, y_c)

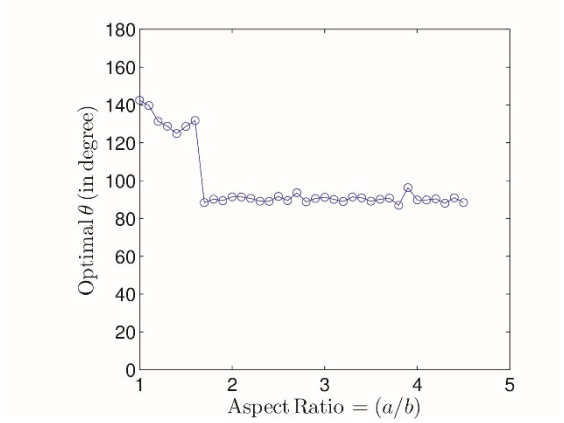

(b) Optimal θ values

Fig. 8 Optimal positions of the elliptical cutout within the cross-ply (0°/90°)$_{2s}$ laminated plate

$(0^{\circ}/90^{\circ})_{2s}$ laminated plate the elliptical cutout should be placed vertically in order to get the maximum buckling load. However, results below will show that this does not remain valid for an angle-ply $(30^{\circ}/-60^{\circ})_{2s}$ laminated plate.

5.2.2 Angle-ply laminates

For angle-ply $(30^{\circ}/-60^{\circ})_{2s}$ laminates, the geometrical parameters of the plate and the cutouts are kept same as described in Section 5.2.1 for the cross-ply $(0^{\circ}/90^{\circ})_{2s}$ laminates. The optimal locations (x_c, y_c) and the

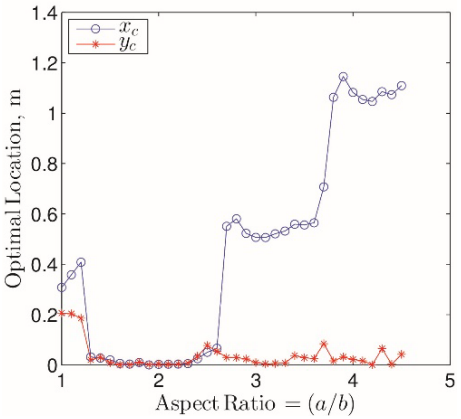

(a) Optimal center locations (x_c, y_c)

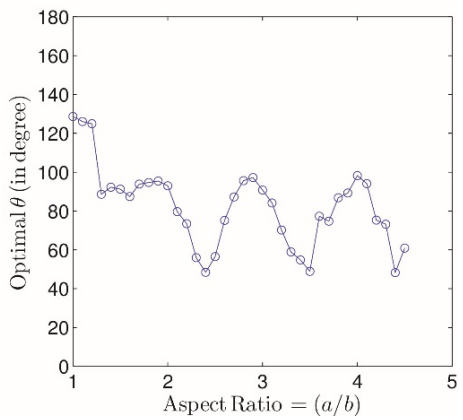

(b) Optimal θ values

Fig. 9 Optimal positions of the elliptical cutout within the angle-ply (30°/-60°)$_{2s}$ laminated plate

corresponding optimal θ values of the elliptical cutout for various values of the plate aspect ratio are shown in Figs. 9(a) and (b) respectively. Tabulated results, for this case, are also given in Table 4 in Appendix B. Interestingly, for the angle-ply laminates considered here, the optimal θ values are not close to 0° or 90° instead it has a variation from 40° to 130° as shown in Fig. 9(b). This shows that for designing elliptical cutout within an orthotropic plate the cutout orientation plays a significant role in order to maximize the buckling load.

To show that the reported optimal positions for the elliptical cutout correspond to the maximum buckling load, we compute the normalized buckling factor (NBF) by keeping the cutout at various positions within the plate and compare them with the optimal results. We consider five positions of the cutout and the comparison is shown in Figs. 10(a) and (b) for the cross-ply $(0^{\circ}/90^{\circ})_{2s}$ and angle-ply $(30^{\circ}/-60^{\circ})_{2s}$ laminates respectively. The figure shows that the N_{xcr} is higher at the optimal cutout position for both the cross-ply and angle-ply laminated plate. These plots also demonstrate that the position of the elliptical cutout has profound effect on the critical buckling load.

5.3 Effect of cutout size

In this section, we discuss the effect of size of the cutout on its optimal location for the maximum buckling loads. We consider two cases to demonstrate this size effect. First, a cross-ply $(0^{\circ}/90^{\circ})_{2s}$ laminated plate having different circular cutouts of radii c = e = 0.1, 0.15, and 0.2 m are considered. The optimal x_c values for these three cutout sizes are given in Fig. 11(a).

Second, we consider angle-ply $(30^{\circ}/-60^{\circ})_{2s}$ laminated plate and three elliptical cutouts of dimensions c = 0.14, 0.21, and 0.28 m with e = 0.5c. Fig. 11(b) shows the optimal x_c values for these three elliptical cutout sizes. These two figures show that the cutout size has significant influence on the optimal results. Therefore, in order to get the optimal design of the plate, the geometry of the cutout has to be selected and then the optimal position has to be computed using the optimization scheme described in this article.

5.4 Effect of material orthotropy

Nature of orthotropy plays a significant role on

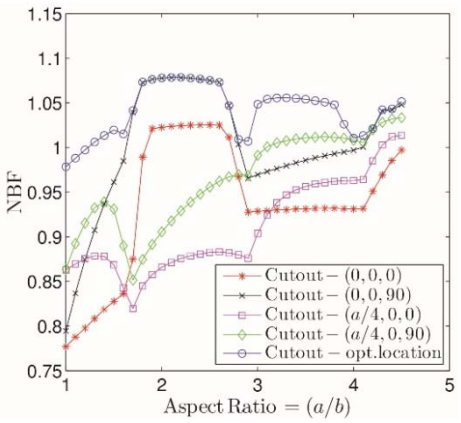

(a) Cross-ply (0°/90°)$_{2s}$ laminated plate

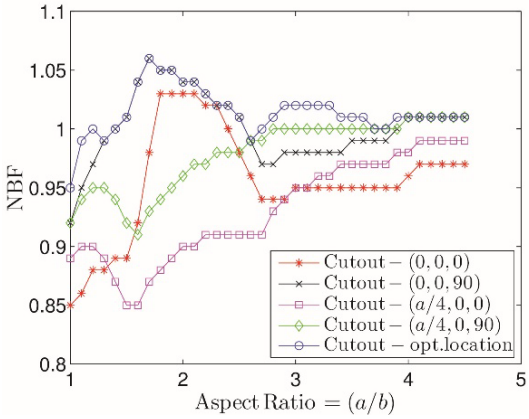

(b) Angle-ply (30°/-60°)$_{2s}$ laminated plate

Fig. 10 Normalized buckling factor (NBF) for five different positions (x_c, y_c, θ) of the elliptical cutout

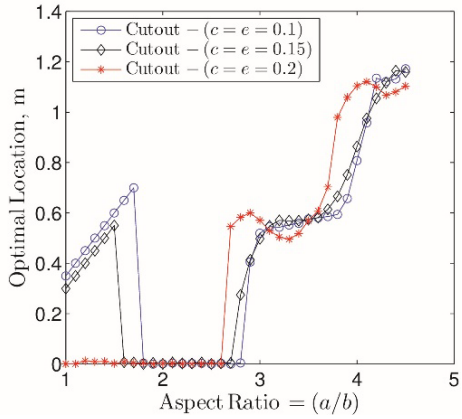

(a) Optimal x_c values for three different circular cutouts within the cross-ply (0°/90°)$_{2s}$ laminated plate

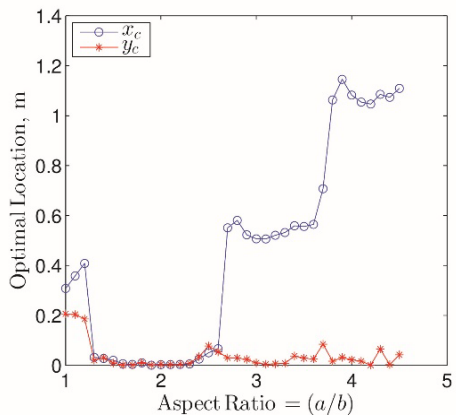

(b) Optimal x_c values for different elliptical cutouts within the angle-ply (30°/-60°)$_{2s}$ laminated plate

Fig. 11 Effect of cutout sizes on the optimal location

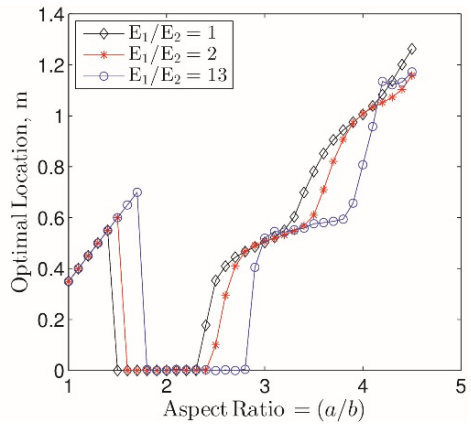

(a) Optimal x_c values for three different Young's modulus ratios

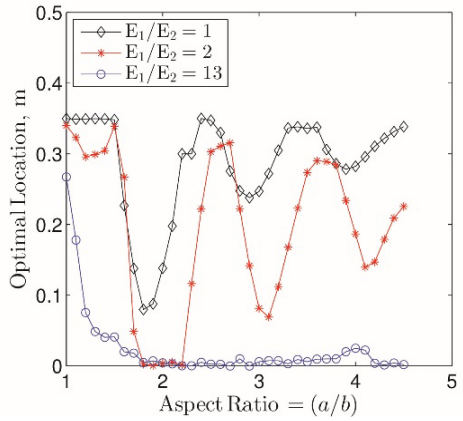

(b) Optimal y_c values for three different Young's modulus ratios

Fig. 12 Effect of material orthotropy on the optimal location of circular cutouts within the cross-ply $(0°/90°)_{2s}$ laminated plate

determining the optimal locations of the cutout. The variation of optimal x_c and y_c values for a circular cutout within the cross-ply $(0^{\circ}/90^{\circ})_{2s}$ laminated plate for three different Young's modulus ratios are shown in Fig. 12. In these plots, only the E_2 values are changed keeping all other material properties same as in Table 1. Fig. 12 shows that the optimal results are significantly different when the stiffness values of the lamina are varied.

6. Conclusions

This paper began with an objective to investigate systematically the optimal position of both circular and elliptical cutouts within an orthotropic plate that gives maximum buckling strengths. To accomplish that we have developed a MATLAB based optimization scheme coupled with buckling computation in ANSYS. The present study is limited to thin orthotropic plate subjected to uniformly distributed edge compression and the linear elastic buckling behavior of the plate is considered.

From this study, the following conclusions are made.

- Both location and orientation of the cutout has profound effect on the buckling load of the orthotropic plate. The presence of cutout redistributes the in-plane stresses in the orthotropic plate and mostly results in the significant reduction of the buckling strength. Therefore, finding the optimal position of the cutouts, using some optimization scheme as presented in this article, would be an important task in the design phases of the orthotropic plates. Optimal results presented in this paper are typical examples of these kinds of studies.
- The geometry of the plate greatly influences the optimal position of the cutout. As the plate aspect ratio changes the optimal positions of the cutouts changes significantly. It has been shown that the optimal position of the cutout for some aspect ratios remains on the nodal lines whereas for other aspect ratios it moves far from the nodal lines. Therefore, the optimal positions of the cutouts may not be intuitively guessed by some prior judgments rather it should be obtained systematically by using some optimization method as illustrated in this paper.
- Nature of material orthotropy has notable effect on the optimal results. The results vary significantly as laminate sequence and material properties of the orthotropic plate changes.
- The shape and size of the cutout has significant effect on the optimal cutout position. Thereby, the optimal position cannot be treated same for different shapes and sizes of the cutout.
- There are some studies available in the literature (e.g., Qablan *et al*. 2009, Narayana *et al*. 2013) where the effect of cutout location on buckling strength has been obtained by just positioning the cutouts in a few selected locations in FEM softwares. Hence, these studies had limitations and the true optimal positions could not be obtained. In contrast to these studies, we could provide the true optimal results in tabular forms and presented a quantitative understanding of the optimal positions of the cutout.

The above conclusions and recommendations are important in design perspective and should be considered in the design phases of the orthotropic plates against buckling failure.

Acknowledgments

Authors would like to thank the Science and Engineering Research Board, Government of India, for financial support (Grant No.: ECR/2016/000964) for this work.

A. APDL used for the buckling analysis

! This APDL is written in a compact form using '$' symbol

```
! Here, MATLAB routine supplies the (xc, yc, theta) values
/CLEAR, START $ /FILNAME, buckling_run $ /PREP7
length=2.8 $ height=1 $ size_elm=35
a1= 0.14 $ a2= 0.07 $ xc = 0.2 $ yc= 0.1 $ theta = 60
BLC5,,,length,height
CYL4,0,0,a1$ARSCALE,2,,,,a2/a1,,,,1
CSYS,1 $ AGEN,,2,,,,theta,,,,1
CSYS,0 $ AGEN,,2,,,xc,yc,,,,1 $ ASBA,1,2,,,
MPTEMP, 1, 0
MPDATA,EX,1,,130e9$MPDATA,EY,1,,10e9
MPDATA,EZ,1,,10e9$MPDATA,PRXY,1,,0.35
MPDATA,PRXY,1,,0.35$ MPDATA,PRXY,1,,0.49
MPDATA,GXY,1,,5e9$MPDATA,GYZ,1,,5e9
MPDATA,GXZ,1,,5e9
```

Table 4 Optimal results for circular (0.1 m radius) and elliptical cutout (c = 0.141 m with e = 0.5c) within the cross-ply $(0°/90°)_{2s}$ and angle-ply $(30°/-60°)_{2s}$ laminated plate. Optimal orientation (θ) values are given in degree

a/b	Circular cutout						Elliptical cutout							
	Cross-ply			Angle-ply			Cross-ply				Angle-ply			
	xc/b	yc/b	NBF	xc/b	yc/b	NBF	xc/b	yc/b	θ	NBF	xc/b	yc/b	θ	NBF
1.0	0.35	0.27	0.96	0.35	0.10	0.97	0.31	0.28	143	0.98	0.31	0.21	129	0.95
1.1	0.40	0.18	0.97	0.4	0.03	0.99	0.36	0.27	140	0.99	0.36	0.20	126	0.99
1.2	0.45	0.08	0.99	0.45	0.00	0.99	0.41	0.22	131	1.00	0.41	0.18	125	1.00
1.3	0.50	0.05	1.00	0.50	0.00	1.00	0.46	0.21	129	1.01	0.05	0.03	89	0.99
1.4	0.55	0.04	1.00	0.55	0.01	0.99	0.51	0.17	125	1.01	0.03	0.03	92	1.00
1.5	0.60	0.04	1.01	0.60	0.00	0.97	0.56	0.18	129	1.02	0.03	0.01	91	1.01
1.6	0.65	0.02	1.00	0.02	0.01	0.97	0.61	0.21	132	1.02	0.01	0.00	87	1.04
1.7	0.70	0.02	0.95	0.00	0.00	1.04	0.01	0.02	88	1.04	0.00	0.00	94	1.06
1.8	0.00	0.00	1.04	0.00	0.00	1.04	0.01	0.01	90	1.07	0.01	0.01	95	1.05
1.9	0.00	0.01	1.04	0.00	0.00	1.04	0.00	0.00	89	1.08	0.00	0.00	95	1.05
2.0	0.00	0.00	1.04	0.01	0.01	1.03	0.01	0.00	91	1.08	0.00	0.00	93	1.04
2.1	0.00	0.00	1.04	0.00	0.00	1.03	0.01	0.00	91	1.08	0.00	0.00	80	1.04
2.2	0.00	0.00	1.04	0.00	0.01	1.03	0.00	0.00	91	1.08	0.00	0.00	73	1.03
2.3	0.00	0.00	1.04	0.00	0.01	1.02	0.01	0.00	89	1.08	0.01	0.01	56	1.02
2.4	0.00	0.01	1.04	0.00	0.00	1.02	0.00	0.00	89	1.08	0.03	0.04	48	1.02
2.5	0.00	0.00	1.04	0.00	0.00	1.00	0.00	0.00	92	1.08	0.05	0.08	57	1.01
2.6	0.00	0.00	1.04	0.00	0.00	0.98	0.01	0.00	89	1.07	0.07	0.05	75	0.99
2.7	0.00	0.00	1.03	0.41	0.00	0.97	0.00	0.02	94	1.05	0.55	0.03	87	1.00
2.8	0.00	0.01	0.98	0.49	0.01	0.99	0.30	0.01	89	1.01	0.58	0.03	96	1.01
2.9	0.41	0.00	0.97	0.53	0.03	1.01	0.50	0.01	91	1.01	0.52	0.02	97	1.02
3.0	0.52	0.01	1.01	0.52	0.01	1.02	0.58	0.01	91	1.05	0.51	0.01	91	1.02
3.1	0.55	0.01	1.03	0.53	0.02	1.02	0.54	0.00	90	1.05	0.51	0.00	84	1.02
3.2	0.54	0.01	1.03	0.53	0.01	1.02	0.55	0.01	89	1.06	0.52	0.01	70	1.02
3.3	0.55	0.00	1.03	0.54	0.01	1.01	0.54	0.00	91	1.06	0.53	0.01	59	1.02
3.4	0.56	0.01	1.03	0.54	0.02	1.01	0.55	0.00	91	1.06	0.56	0.04	55	1.01
3.5	0.58	0.01	1.03	0.58	0.01	1.01	0.55	0.00	89	1.05	0.56	0.03	49	1.01
3.6	0.58	0.01	1.03	0.64	0.00	1.00	0.56	0.01	90	1.05	0.56	0.03	77	1.01
3.7	0.59	0.01	1.03	0.64	0.01	0.99	0.56	0.01	91	1.05	0.71	0.08	75	1.00
3.8	0.59	0.01	1.03	0.74	0.01	0.99	0.55	0.01	87	1.05	1.06	0.02	87	1.00
3.9	0.66	0.02	1.01	0.96	0.01	1.00	0.63	0.02	96	1.03	1.15	0.03	89	1.01
4.0	0.81	0.03	1.00	1.04	0.00	1.00	0.84	0.01	90	1.01	1.08	0.02	98	1.01
4.1	0.96	0.02	0.99	1.08	0.00	1.01	1.19	0.00	90	1.01	1.05	0.02	94	1.01
4.2	1.13	0.00	1.01	1.07	0.01	1.01	1.13	0.00	90	1.02	1.05	0.00	75	1.01
4.3	1.12	0.00	1.02	1.07	0.00	1.01	0.00	0.01	88	1.04	1.09	0.07	73	1.01
4.4	1.13	0.00	1.02	1.08	0.00	1.01	0.00	0.00	91	1.04	1.07	0.00	48	1.01
4.5	1.17	0.00	1.02	1.10	0.01	1.01	0.00	0.01	88	1.05	1.11	0.04	61	1.01

```
Sect, 1, shell,
Secdata, 0.15e-3, 1, 0.0,3 $ secdata, 0.15e-3, 1,90,3
Secdata, 0.15e-3, 1, 0.0,3 $ secdata, 0.15e-3, 1,90,3
Secdata, 0.15e-3, 1,90,3 $ secdata, 0.15e-3, 1, 0, 3
Secdata, 0.15e-3, 1,90,3 $ secdata, 0.15e-3, 1, 0.0,3
Secoffset, MID $ seccontrol, , , , , , ,
ET, 1, SHELL181 $ KEYOPT, 1, 3, 0
LDIV,2,0.5,,2,0 $ LDIV,4,0.5,,2,0
LESIZE,ALL,height/size_elm/1.5
LESIZE, 1, height/size_elm $ LESIZE, 2, height/size_elm
LESIZE, 3, height/size_elm $ LESIZE, 4, height/size_elm
LESIZE, 9, height/size_elm $ LESIZE, 10, height/size_elm
AMESH, ALL $CSKP,11,0,1,2,3 $ EMODIF,ALL,ESYS,11
LSEL,S,LINE,,1 $ LSEL,A,LINE,,2 $ LSEL,A,LINE,,3
LSEL,A,LINE,,4 $ LSEL,A,LINE,,9 $ LSEL,A,LINE,,10
NSLL, S, 1 $ D, ALL, UZ $ ALLS

KSEL, S, KP,, 10 $ NSLK,S $ D,ALL,UX $ D,ALL,UY $
ALLS
KSEL, S, KP,, 9 $ NSLK,S $ D,ALL,UY $ ALLS
LSEL,S,LINE,,2 $ LSEL,A,LINE,,4 $ LSEL,A,LINE,,9
LSEL, A, LINE,,10 $ SFL,ALL,PRES,10 $ ALLS
/SOLU $ ANTYPE, STATIC $ PSTRES, ON $ SOLVE $
FINISH
/SOLU $ ANTYPE, BUCKLE $ BUCOPT, LANB, 1 $
SOLVE $ FINISH
/POST1 $ RSYS, SOLU $ FILE, buckling_run, rst $ SET,
1, 1
*GET, factor, ACTIVE, 0, SET, FREQ,
/OUT, buck_fact, dat
*vwrite, 1, factor
(F4.1, 2X, F10.4)
/OUT
SAVE
FINISH
```

B. Tabulated optimal results for circular and elliptical cutouts

Optimal locations for the circular and elliptical cutouts within the cross-ply $(0^{\circ}/90^{\circ})_{2s}$ and angle-ply $(30^{\circ}/-60^{\circ})_{2s}$ laminated plate for various values of plate aspect ratios are shown in Table 4.

References

Adali, S., Lene, F., Duvaut, G. and Chiaruttini, V. (2003), "Optimization of laminated composites subject to uncertain buckling loads", *Compos. Struct.*, **62**(3-4), 261-269.

Aktas, M. and Balcioglu, H.E. (2014), "Buckling behavior of pultruded composite beams with circular cutouts", *Steel Compos. Struct., Int. J.*, **17**(4), 359-370.

Al Qablan, H., Katkhuda, H. and Dwairi, H. (2009), "Assessment of the buckling behavior of square composite plates with circular cutout subjected to in-plane shear", *Jordan J. Civil Eng.*, **3**(2), 184-195.

Altunsaray, E. and Bayer, I. (2014), "Buckling of symmetrically laminated quasi-isotropic thin rectangular plates", *Steel Compos. Struct., Int. J.*, **17**(3), 305-320.

Anil, V., Upadhyay, C.S. and Iyengar, N.G.R. (2007), "Stability analysis of composite laminate with and without rectangular cutout under biaxial loading", *Compos. Struct.*, **80**(1), 92-104.

ANSYS Inc. (2015), ANSYS Reference Manual, Release 15.0 Documentation for ANSYS.

Baba, B.O. (2007), "Buckling behavior of laminated composite plates", *J. Reinf. Plast. Compos.*, **26**(16), 1637-1655.

Baba, B.O. and Baltaci, A. (2007), "Buckling characteristics of symmetrically and antisymmetrically laminated composite plates with central cutout", *Appl. Compos. Mater.*, **14**(4), 265-276.

Baltaci, A., Sarikanat, M. and Yildiz, H. (2006), "Buckling analysis of laminated composite circular plates with holes", *J. Reinf. Plast. Compos.*, **25**(7), 733-744.

Baseri, V., Jafari, G.S. and Kolahchi, R. (2016), "Analytical solution for buckling of embedded laminated plates based on higher order shear deformation plate theory", *Steel Compos. Struct., Int. J.*, **21**(4), 883-919.

Darvizeh, M., Darvizeh, A. and Sharma, C.B. (2002), "Buckling analysis of composite plates using differential quadrature method (DQM)", *Steel Compos. Struct., Int. J.*, **2**(2), 99-112.

Ghannadpour, S.A.M., Najafi, A. and Mohammadi, B. (2006), "On the buckling behavior of cross-ply laminated composite plates due to circular/elliptical cutouts", *Compos. Struct.*, **75**(1-4), 3-6.

Goldberg, D.E. (2005), "Genetic algorithms in search, optimization, and machine learning", Pearson Education Inc.

Jain, P. and Kumar, A. (2004), "Postbuckling response of square laminates with a central circular/elliptical cutout", *Compos. Struct.*, **65**(2), 179-185.

Jana, P. (2016), "Optimal design of uniaxially compressed perforated rectangular plate for maximum buckling load", *Thin-Wall. Struct.*, **103**, 225-230.

Komur, M.A. (2011), "Elasto-plastic buckling analysis for perforated steel plates subject to uniform compression", *Mech. Res. Commun.*, **38**(2), 117-122.

Komur, M.A. and Sonmez, M. (2008), "Elastic buckling of rectangular plates under linearly varying in-plane normal load with a circular cutout", *Mech. Res. Commun.*, **35**(6), 361-371.

Komur, M.A., Sen, F., Atas, A. and Arslan, N. (2010), "Buckling analysis of laminated composite plates with an elliptical/circular cutout using FEM", *Adv. Eng. Software*, **41**(2), 161-164.

Kumar, D. and Singh, S.B. (2010), "Effects of boundary conditions on buckling and postbuckling responses of composite laminate with various shaped cutouts", *Int. J. Mech. Sci.*, **92**(3), 769-779.

Larsson, P.L. (1987), "On buckling of orthotropic compressed plates with circular holes", *Compos. Struct.*, **7**(2), 103-121.

Lee, Y.J., Lin, H.J. and Lin, C.C. (1989), "A study on the buckling behavior of an orthotropic square plate with a central circular hole", *Compos. Struct.*, **13**(3), 173-188.

Leissa, A.W. (1987), "A review of laminated composite plate buckling", *Appl. Mech. Rev.*, **40**(5), 575-591.

Lin, C.C. and Kuo, C.S. (1989), "Buckling of laminated plates with holes", *J. Compos. Mater.*, **23**(6), 536-553.

Lopatin, A.V. and Morozov, E.V. (2014), "Approximate buckling analysis of the CCFF orthotropic plates subjected to in-plane bending", *Int. J. Mech. Sci.*, 85, 38-44.

Mohammadi, B., Najafi, A. and Ghannadpour, S.A.M. (2006), "Effective widths of compression-loaded of perforated cross-ply laminated composites", *Compos. Struct.*, **75**(1-4), 7-13.

Narayana, A.L., Rao, K. and Kumar, R.V. (2013), "Effect of location of cutout and plate aspect ratio on buckling strength of rectangular composite plate with square/rectangular cutout subjected to various linearly varying in-plane loading using FEM", *Int. J. Mech.*, **7**(4) , 508-513.

Nemeth, M.P. (1988), "Buckling behavior of compression-loaded symmetrically laminated angle-ply plates with holes", *AIAA Journal*, **26**(3), 330-336.

Onkar, A.K., Upadhyay, C.S. and Yadav, D. (2007), "Stochastic finite element buckling analysis of laminated plates with circular cutout under uniaxial compression", *J. Appl. Mech.*, **74**(4), 798-809.

Paluch, B., Grediac, M. and Faye, A. (2008), "Combining a finite element programme and a genetic algorithm to optimize composite structures with variable thickness", *Compos. Struct.*, **83**(3), 284-294.

Rajanna, T., Banerjee, S., Desai, Y.M. and Prabhakara, D.L. (2016), "Vibration and buckling analyses of laminated panels with and without cutouts under compressive and tensile edge loads", *Steel Compos. Struct., Int. J.*, **21**(1), 37-55.

Reddy, J.N. (2003), "Mechanics of Laminated Composite Plates and Shells: Theory and Analysis", CRC Press.

Seifi, R., Chahardoli, S. and Attar, A.A. (2017), "Axial buckling of perforated plates reinforced with strips and middle tubes", *Mech. Res. Commun.*, **85**, 21-32.

Sharma, D.S., Patel, N.P. and Trivedi, R.R. (2014), "Optimum design of laminates containing an elliptical hole", *Int. J. Mech. Sci.*, **85**, 76-87.

Sivakumar, K., Iyengar, N.G.R. and Deb, K. (1998), "Optimum design of laminated composite plates with cutouts using a genetic algorithm", *Compos. Struct.*, **42**(3), 265-279.

Spallino, R. and Rizzo, S. (2002), "Multi-objective discrete optimization of laminated structures", *Mech. Res. Commun.*, **29**(1), 17-25.

Srivatsa, K.S. and Murty, A.K. (1992), "Stability of laminated composite plates with cut-outs.", *Comput. Struct.*, **43**(2), 273-279.

Topal, U. and Uzman, Ü. (2007), "Optimum design of laminated composite plates to maximize buckling load using MFD method", *Thin-Wall. Struct.*, **45**(7-8), 660-669.

Walker, M. (1999), "Optimal design of symmetric laminates with cut-outs for maximum buckling load", *Comput. Struct.*, **70**(3), 337-343.

Zehnder, N. and Ermanni, P. (2006), "A methodology for the global optimization of laminated composite structures", *Compos. Struct.*, **72**(3), 311-320.

Zhang, Y.X. and Yang, C.H. (2009), "Recent developments in finite element analysis for laminated composite plates", *Compos. Struct.*, **88**(1), 147-157.

Zhong, H. and Gu, C. (2007), "Buckling of symmetrical cross-ply composite rectangular plates under a linearly varying in-plane load", *Compos. Struct.*, 80(1), 42-48.

CC